



Lasers in Manufacturing Conference 2023

# Challenges in the development of the Laser Metal Deposition process for use in microgravity at the Einstein-Elevator

Marvin Raupert<sup>a,\*</sup>, Emre Tahtali<sup>a</sup>, Richard Sperling<sup>a</sup>, Alexander Heidt<sup>a</sup>,  
Christoph Lotz<sup>a</sup>, Ludger Overmeyer<sup>b</sup>

<sup>a</sup>Leibniz Universität Hannover, Institut für Transport- und Automatisierungstechnik, c/o Hannover Institute of Technology,  
Callinstraße 36, 30167 Hannover, Germany

<sup>b</sup>Leibniz Universität Hannover, Institut für Transport- und Automatisierungstechnik, An der Universität 2,  
30823 Garbsen, Germany

---

## Abstract

This paper is about the challenges in developing the Laser Metal Deposition process with metal powder for use in microgravity. The modified gravitational conditions are set up for a few seconds using a drop tower, the *Einstein-Elevator* of the *Leibniz University Hannover*. In addition to the drop tower, the specially adapted setup of the experiment will be explained. The samples produced in microgravity during this project will demonstrate the influence of gravity on this additive manufacturing process and on the materials used. Thermal analyses using the Ansys software show how the temperature distribution of the manufactured specimens looks over time and what this means for the execution of the experiment.

Keywords: Laser Metal Deposition; microgravity; drop tower; Einstein-Elevator; Additive Manufacturing; thermal analysis

---

## 1. Introduction

Laser Metal Deposition (LMD) with metal powder is one example of a free-form additive manufacturing process. In addition to production of near-net-shape parts, coating, joining and feature addition, the technique can also be used to repair existing components. Due to these unique properties, the process has

---

\* Corresponding author. Tel.: +49(0)511-762-14823; fax: +49(0)511-762-4007.  
E-mail address: marvin.raupert@ita.uni-hannover.de.

enormous potential on earth as well as in extraterrestrial applications. Of particular interest is the manufacturing in microgravity during longer space missions [Mahamood, 2018].

The development of the LMD with metal powder for environmental conditions in space is being researched at the *Einstein-Elevator* of Leibniz University Hannover. This third-generation drop tower is capable of performing a vertical parabolic flight [Reitz et al., 2021]. During this time, the experiment is in free fall and LMD manufacturing can take place under microgravity. The samples to be fabricated are cylinders 3 mm in diameter and 100 mm high (called seed sticks). Their geometry refers to DIN EN ISO 6892-1:2017-02, allowing all samples to be analyzed and compared with each other afterwards. In this research project, the two materials commonly used in aerospace engineering are Inconel 625 (nickel-chromium-molybdenum-niobium alloy) and Ti-6Al-4V (Ti64), whereby only Ti64 is considered in more detail in this paper. Furthermore, the challenges of integrating the LMD setup into the *Einstein-Elevator* and the development of the process for use in microgravity under special environmental conditions are highlighted. In particular, thermal transient analyses show how the temperature distribution in the sample and the substrate plate evolves over time and what significance this has for the manufacturing process.

## 2. Experiment setup

In this chapter, the entire experimental setup required for manufacturing the seed sticks in microgravity by the LMD method is explained step by step. First, it is shown which earth-bound facility can be used to generate microgravity for this experiment. Subsequently, the properties of this facility and the requirements for the experiment setup will be explained. Finally, it will be shown how the experimental setup was adapted to the environmental conditions and how the manufacturing of the seed sticks is implemented.

### 2.1. Einstein-Elevator

The *Einstein-Elevator* is a drop tower of the Leibniz University Hannover (LUH), shown in figure 1. Located at the *Hannover Institute of Technology (HITec)*, the facility allows experiments to be conducted under different gravity conditions from microgravity to hypergravity (up to 5 *g*). In the case of a microgravity flight, 4 seconds are available for the experiment. For this purpose, the experiment is accelerated with 5 *g*, taken into free fall, and then decelerated again with approximately 5 *g*. The next flight can be started after a 4-minute break to recharge the energy storage and to cool down different components. Relative to other facilities, the *Einstein-Elevator* is characterized by a unique design that enables the implementation of large scale experimental setups (1.7 m in diameter, a height of 2 m and a weight of up to 1,000 kg) at a high repetition rate, allowing up to 100 experiments to be performed in an eight-hour shift. This makes it possible to collect statistical measurement data. [Lotz, 2022 and Lotz et al., 2023]

The structure of the *Einstein-Elevator* can be divided into the three main components gondola (a vacuum chamber made of carbon fiber-reinforced plastic), drive and guidance system (see figure 2). In this case, the experiment capsule is not dropped in an evacuated room. At the *Einstein-Elevator* the experiment setup is located in the experiment carrier system inside the gondola, which in turn is actively driven and guided in two completely decoupled support structures. The outer structure guides the gondola and the inner structure is responsible for the drive. Therefore linear synchronous motors are placed over the whole length of the tower. Each supporting structure rests on its own foundation to prevent vibrations from the outer system and the transmission of vibrations from the drive system to the gondola guide system. The only connection between the drive and the guide components with the gondola consists of a single coupling rod. The structure of the *Einstein-Elevator* is shown in figure 2. [Lotz et al., 2014 and Lotz et al., 2018]



Fig. 1. The *Einstein-Elevator* with the experiment carrier (Photo: Leibniz University Hannover/Marvin Raupert).

In comparison to microgravity flights, the experiment carrier is attached to the gondola for gravity conditions in the range of  $\mu g$  to  $1 g$  (hypogravity) and  $1 g$  to  $5 g$  (hypergravity). For these conditions, an adjusted trajectory is created to generate the required acceleration. The duration of the test depends on the desired acceleration. [Lotz, 2022]

## 2.2. Experiment carrier

A new experiment carrier for the *Einstein-Elevator* is currently being developed, which will also integrate the research project presented in this publication. The platform is modularly designed so that it can be adapted for a wide variety of experiment setups. By integrating the new advanced carrier system, very low residual accelerations of less than  $1 \mu g$  can be achieved while maintaining a maximum payload volume. This is made possible, among other things, by the build-up of a vacuum inside the gondola. Thus, in case of a microgravity flight, the experiment setup is not only mechanically but also acoustically decoupled.

First of all, the setup of the experiment carrier consists of the base, in which all the necessary hardware for controlling the carrier is integrated and which stands on the floor of the gondola when the facility (*Einstein-Elevator*) is at parking position. The payload of the experiments is placed on special levels. The number of installed levels as well as their distances to each other and to the base can be adjusted individually. All cables and connections can be routed through cutouts in the levels. For experiments that cannot be set up in a vacuum, a pressure-tight shell can optionally be placed on the base to separate the payload volume from the environment (vacuum). Atmospheres of different composition can be set up inside the pressure-tight shell.

The experiment carrier is equipped with several features. These include an active cooling system with a capacity of  $1 \text{ kW}$  and the ability to record basic telemetry data. For this purpose, different sensors record data on the triaxial acceleration, the rotation rate of the carrier, the magnetic field inside the carrier and the temperature and pressure at different locations. A  $24 \text{ V DC}$  power supply with a capacity of  $400 \text{ W}$  and, if required, a  $230 \text{ V AC}$  power supply are available for the experiments. For permanent control and monitoring

of the experiment, there is also a network connection for the experiment hardware, which is routed to the outside via optical data couplers. [Raupert et al., 2022]

### 2.3. Setup of the LMD process

This sub-section focuses on the setup of the LMD process, which takes place at two levels of the experiment carrier and is shown in figure 2. To maximize the number of seed sticks to be produced automatically one after the other without having to open the gondola of the drop tower between flights, the setup has been adapted accordingly. The manufacturing process is carried out within a process chamber at the second level during the microgravity time of the vertical parabolic flight at the *Einstein-Elevator*. In this process, the seed sticks are produced on a sample plate that is connected to a rotary table and a linear axis. During the production of a seed stick, the sample plate is moved vertically downwards. As soon as a seed stick has been produced, the sample plate rotates and moves back to the upper starting position. Since the physical properties (e.g. the liquidus temperature) of the sample plate (aluminum) and the seed stick are too different, the samples are not printed directly onto the sample plate but onto a steel ring structure fixed in between (see figure 3).

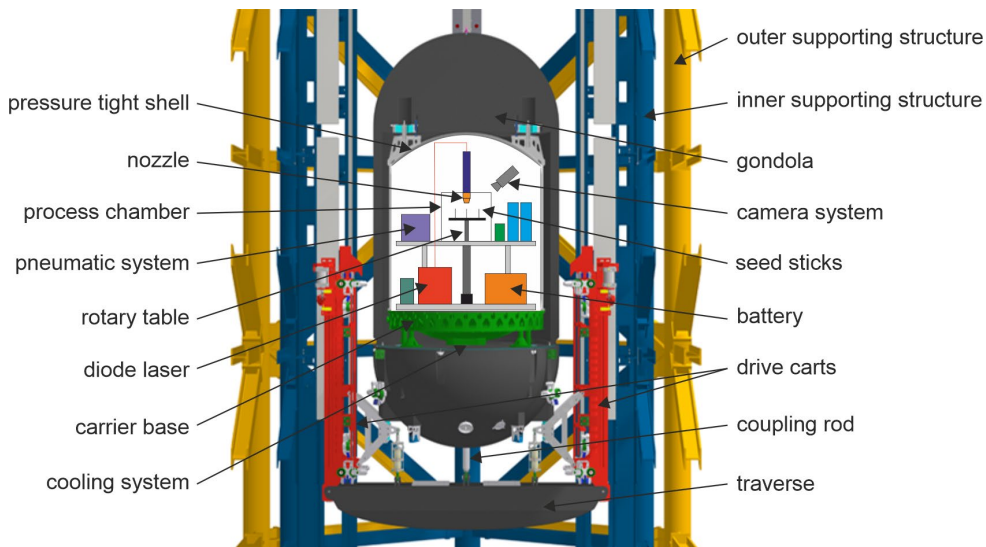


Fig. 2. Experiment setup inside the gondola of the Einstein-Elevator [Raupert et al., 2022].

In this test setup, the LMD nozzle is located inside the process chamber on the ceiling. The laser beam is introduced into the chamber from outside through a protective glass. The electronic connections for the manipulator system and the gas-powder mixture (Ti64 and argon as carrier gas) are fed into the chamber through corresponding flanges. The process takes place under an inert protective gas atmosphere with argon to minimize oxygen and moisture content and ensure safety with respect to dust explosions. In addition, the chamber has two sight glasses mounted at different positions through which the manufacturing process can be observed and analyzed. A high-speed camera and a thermal imaging camera are available for this purpose.

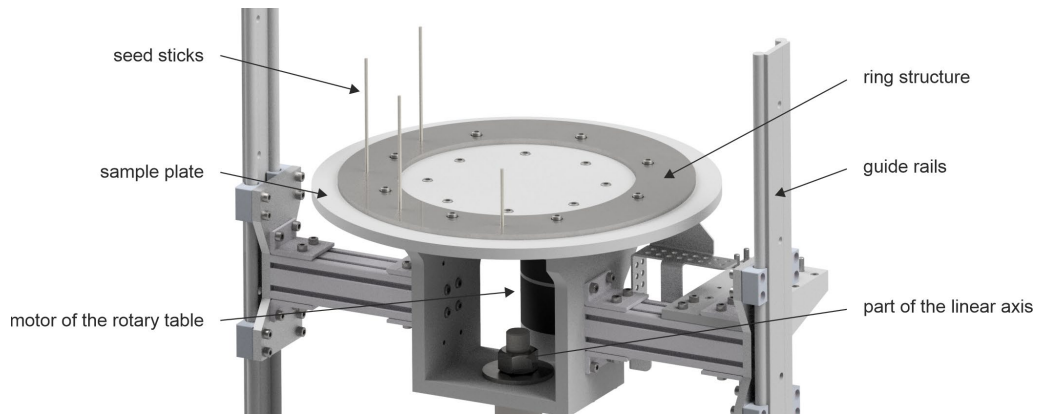


Fig. 3. Experiment setup inside the process chamber.

Outside the process chamber, all other components necessary for the LMD process are placed on both levels, with the larger and mainly heavy components distributed on the first level and the smaller components on the second level. A diode laser with a maximum output power of 2000 W is used to generate the laser beam. The beam quality is 44 mm mrad and the wavelength is in the range of 900 to 1080 nm. An optical fiber with a core diameter of 400  $\mu\text{m}$  and a numerical aperture of 0.22 guides the generated laser beam from the diode laser to the processing optics. Due to the additional cooling power, a total of 6 kW is provided for the diode laser by an energy storage device placed in the first level.

In this experimental setup, the cooling system consists of four circuits with water as the medium, three of which are located inside and one outside the gondola of the *Einstein-Elevator*. Via the heat exchanger integrated in the new experiment carrier, the energy from the manufacturing process is dissipated from the gondola during the standstill periods of the drop tower. The main cooling circuit inside the gondola has a temperature of about 10 °C and is connected to the two bypass circuits via one heat exchanger each. The first bypass is the inner cooling circuit of the diode laser, which maintains a temperature between 10 and 16 °C. The second bypass is responsible for cooling the processing optics and the LMD nozzle. In this case, a temperature of 30 °C is present. To build up the temperatures, further control components as well as components for heating the water are integrated in the circuits.

The metal powder is fed to the melt pool in this LMD process with the aid of a powder conveyor specially developed for microgravity and argon as the carrier gas. Further information on the developed powder conveyor can be found in Raupert et al., 2022. The manufacturing process takes place in the closed gondola and the systems process chamber. Since 1 bar is to be maintained within both systems and the LMD manufacturing process does not have an efficiency of 100 %, argon and the excess metal powder are separated after the process and then stored in containers provided for this purpose. The pneumatic setup is designed in such a way that as many active components as possible, such as motors of pump systems, are not operated during the microgravity time and thus less vibrations are introduced into the system.

### 3. Thermal transient analysis

One of the goals of this research project is to find out how the Laser Metal Deposition process has to be adapted for use in microgravity and what influence gravity then has on the process and the material properties of the manufactured components. In this experimental setup, fabrication takes place within the 4-

second microgravity duration of the *Einstein-Elevator*. Importantly, fabrication in the first step of the investigation only lasts long enough for the molten pool to cool and for all parts of the seed sticks to fall back below the solidus temperature. Once these conditions are met, the seed stick is in solid form and the 5 g deceleration can no longer affect the geometry. For this reason, a thermal transient analysis is performed within this work to investigate how a 3-second manufacturing phase in combination with a 1-second cooling phase affects the process and whether it is sufficient for this experimental setup.

### 3.1. Material properties of Ti-6Al-4V

The high-strength titanium alloy Ti-6Al-4V consists of 6 wt% (weight percent) aluminum and 4 wt% vanadium besides pure titanium. The properties are high strength (tensile strength 950 MPa), low density (solid 4.43 g/cm<sup>3</sup>), good corrosion resistance and high fracture toughness (75 MPa·m<sup>1/2</sup>). This combination makes the material very interesting for the aerospace sector. However, when processing Ti6Al4V, it must also be taken into account that the material has a low thermal conductivity (solid 6.7 W/m/K and liquid 32.5 W/m/K), active chemical reactivity to oxygen and propensity to strain hardening. The solidus temperature is 1604 °C and the liquidus temperature is 1660 °C. [Liu et al., 2019 and Yan et al., 2015]

In addition to aluminum and vanadium, other elements such as carbon, iron, yttrium, hydrogen, oxygen and nitrogen are contained in small quantities. Since titanium is the main component of this alloy, a detailed description of the allotropic element is important. Titanium has two different crystal structures:  $\alpha$ -titanium with hexagonal close-packed (hcp) structure and  $\beta$ -titanium with body centered cubic (bcc) structure. Thereby,  $\alpha$ -titanium exists below and  $\beta$ -titanium above the  $\beta$ -transus-temperature of 980 °C [Yan et al., 2015]. Since aluminum is an  $\alpha$ -titanium stabilizer, while vanadium stabilizes the  $\beta$ -titanium, Ti-6Al-4V holds the  $\alpha$ + $\beta$ -double phase at room temperature. In Ti-6Al-4V, the phase transformation depends strongly on the temperature history, cooling rate and composition. If the cooling rate is slow (<20 °C/s), there is enough time for a diffusion process to occur so that a dual phase of  $\alpha$  and  $\beta$  can form. If the cooling rate is faster,  $\beta$  will be decomposed by a non-equilibrium martensite reaction. In this case, pure martensite will be formed at cooling rates greater than 410 °C/s. At rates in between, both forms will occur. The different microstructures have a major influence on the mechanical properties of the material. [Liu et al., 2019]

### 3.2. Parameter and setup of the simulation

The thermal simulations created in this work have been generated by Ansys Additive Suite software. Part of the tool can be used specifically for Direct Energy Deposition processes, although some simplifications have to be made compared to the real manufacturing process. The components that have a direct impact on heat transfer during seed stick fabrication are incorporated into the thermal transient simulation. These include the seed sticks, the ring structure and the sample plate (see Fig. 3). To minimize the computational effort and since only the fabrication of one seed stick is considered at a time, only 30° pieces of the point-symmetric ring structure and sample plate are included in the simulation. A G-code in the software determines where the seed stick is to be raised on the ring structure. As this tool does not allow the laser power used to be specified, but only the prevailing temperature at the point to be produced (melt pool), a process temperature of 1754 °C is set. Depending on the material selected, it is common for power-controlled Laser Metal Deposition by temperature measurement to set a temperature that is approximately 150 °C above the solidus temperature. It is also not possible in the software to create a fusion zone between Ti6Al4V (seed stick) and steel (ring structure), since the individual building blocks are merely deposited one after the other on the surface of the ring structure. To compensate for this behavior, the production of the seed stick starts in a small recess within the ring structure.

Through the preliminary tests, a growth rate for the production of the seed stick of 2.5 mm/s has proven to be good. In the simulation, this corresponds to a material deposition rate of 17.671 mm<sup>3</sup>/s. The surrounding inert gas atmosphere is argon and the room temperature is 23 °C. In LMD, the metal powder is conveyed to the molten pool using a carrier gas. Another gas stream positioned centrally at the nozzle prevents the particles from moving back to the nozzle. This overall flow is introduced in the simulation by a gas convection coefficient of 100 W/(m<sup>2</sup>·°C). According to Ansys, this corresponds to forced convection with a moderate speed flow. During the standstill periods of 4 minutes each, the convection coefficient approaches zero, since no manufacturing takes place. The remaining parameters are entered into the simulation from the Ansys material database.

### 3.3. Simulation results

The first thermal transient analysis represents the entire manufacturing process of a seed stick. At a printing speed of 2.5 mm/s and a manufacturing time of 3 seconds, 7.5 mm of the sample are manufactured per flight in the *Einstein-Elevator*. After a 4-minute break, the next manufacturing process takes place until the 100 mm target height is reached. Figure 4 shows the maximum prevailing temperatures over time. It can be seen that the seed stick cools down less quickly, since less heat energy can be dissipated into the environment due to the increasingly larger seed stick. The effect is further enhanced by the fact that Ti6Al4V has a low thermal conductivity.

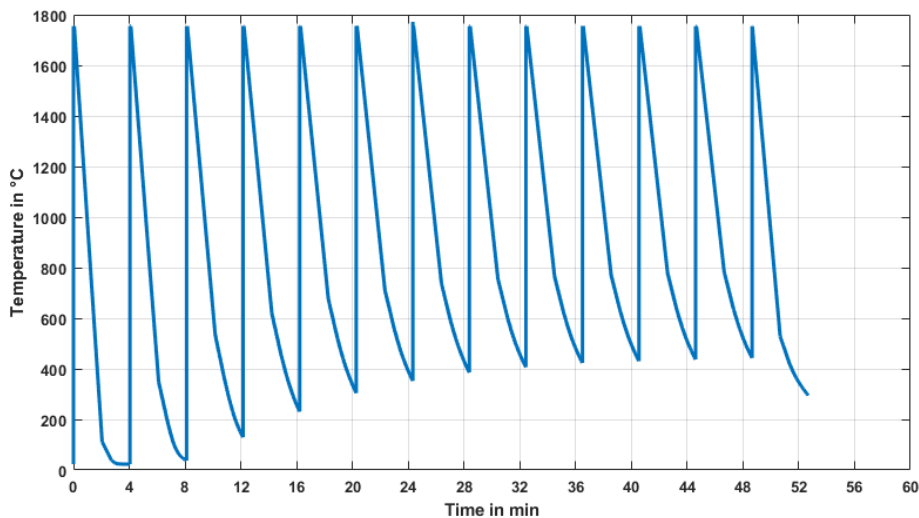


Fig. 4. Maximum temperature over time during manufacturing of a seed stick.

The next two analyses examine the first and last manufacturing cycles of the seed stick again in more detail. In the first analysis of the entire seed stick, it is not possible to view the exact temperature-time curve of the 1-second cooling phase in more detail due to the lack of calculation steps in the DED tool of Ansys. Figure 5 a) therefore shows the temperature distribution of the first production section 4 seconds after manufacturing starts.

After 3-seconds manufacturing and 1-second cooling time, the simulation shows a maximum temperature of 1407.3 °C, which is below the solidus line and thus the deceleration with 5 g can no longer have any effect

on the geometry. The final manufacturing section, shown in figure 5 b), is set with initial parameters from the first analysis to investigate the limiting case. For this purpose, the seed stick, the ring structure and the sample plate are given the temperatures that the components had before the last production step but after the 4-minute break (see figure 4). In this respect, the seed stick is set at 443 °C and the ring structure and sample plate at 25 °C initial temperature.

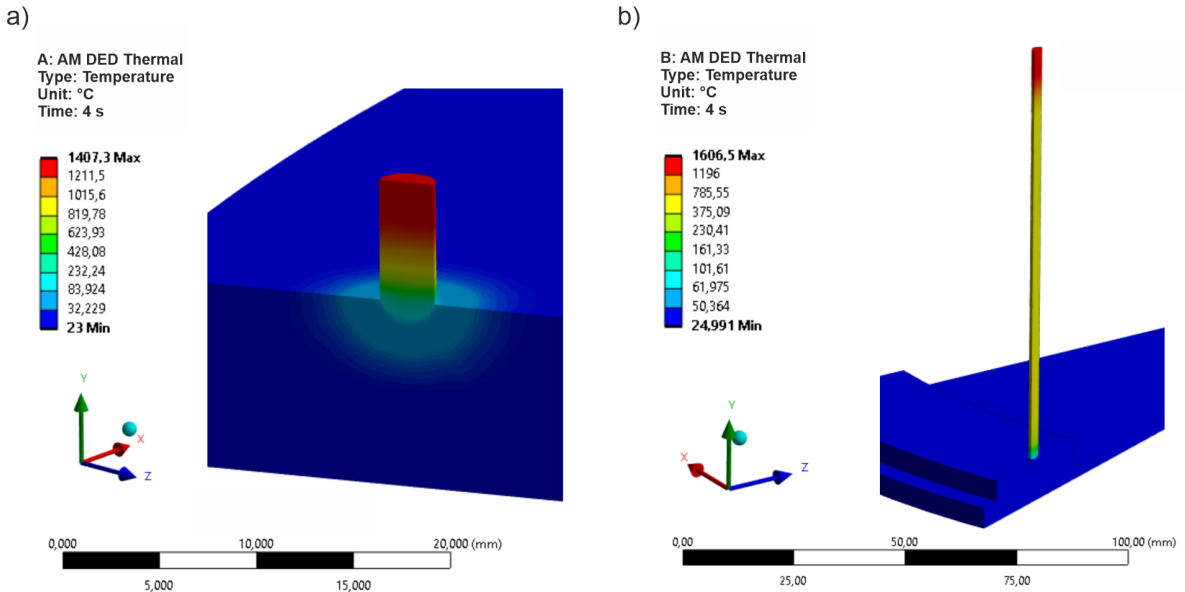


Fig. 5. Temperature distribution after 3-second manufacturing time and 1-second cooling period of the first (a) and the last (b) production section of the seed stick in cross-section.

The results show that for this last section, the maximum prevailing temperature after 3-seconds of manufacturing and 1-second cooling period is 1606.5 °C, which is above the solidus temperature. The taller the seed stick becomes, the shorter the manufacturing time must be during the microgravity period. The exact temperature-time curve of the cooling periods of the first and last production sections are shown in figure 6. The taller the seed stick, the less quickly the thermal energy can be released to the surrounding components. Hence, the production time or the laser power must be adapted to the seed stick height.

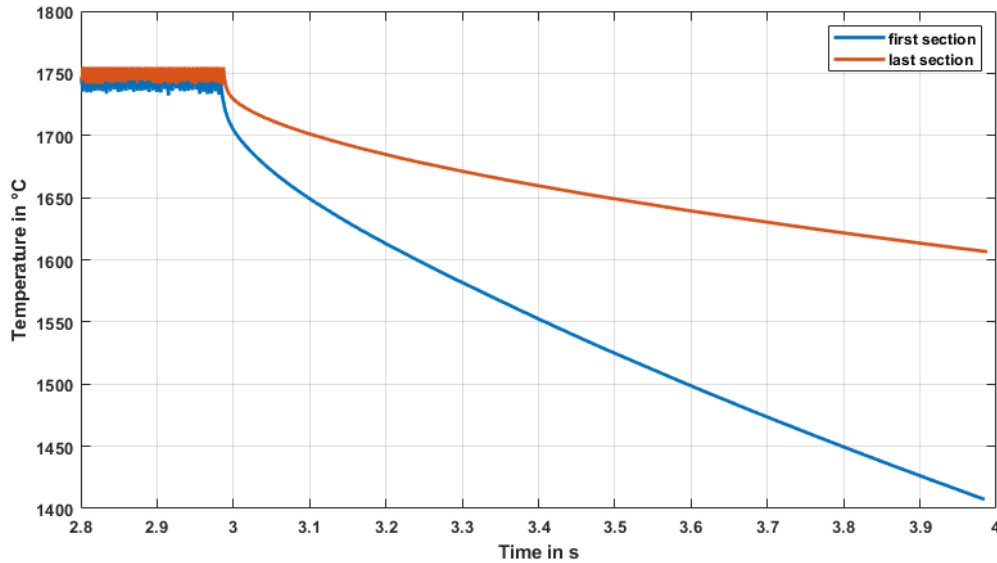


Fig. 6. Maximum temperature-time curve of the cooling periods in the first and last production section.

#### 4. Summary and Outlook

The evaluation of the thermal transient simulation shows that a manufacturing duration of up to 3 seconds is possible during the 4-second microgravity period in the *Einstein-Elevator* in the first manufacturing section of the seed stick. Within the last second, the component cools down to the point where the temperature drops below the solidus line. As a result, the subsequent deceleration of the drop tower with 5 g no longer has any effect on the outer geometry. In the final manufacturing stage of the seed stick, it is evident that the manufacturing time or the laser power must be reduced or adjusted. Due to the advanced height of the seed stick, the thermal energy can be dissipated less quickly to the environment, which means that after the 1-second cooling period, there are still areas above the solidus temperature in the extreme case. Furthermore, it is also possible to additionally cool the relevant components via the argon gas flow within the 4-minute pause, so that the generated thermal energy can be absorbed more quickly during the next manufacturing stage.

A closer look at the material Ti6Al4V shows that even after the solidus temperature, processes still take place in the alloy during the cooling phase. The transformation into  $\alpha$ - and  $\beta$ -titanium as well as different martensite forms depend on the temperature history, cooling rate and composition. Some scientific studies according to Yang et al., 2016 and Wunderlich, 2011 have shown that the gravity prevailing during fabrication also affects the microstructure composition. For a more detailed investigation, the fabrication time and gas flow for cooling should be adjusted so that the maximum prevailing temperature in the component drops at least below the beta-transus-temperature and the transformation processes are completed before deceleration of the drop tower with 5 g starts. It would be of great importance to investigate the relationship between the cooling rate and the gravitation as well as its effect on the composition of the microstructure while keeping the material composition of Ti6Al4V constant.

## Acknowledgements

This research project (project number: 456663377) is funded by the *Deutsche Forschungsgemeinschaft (DFG)*. The authors would like to thank the *DFG* for their financial support. In addition, the authors would like to thank the *DFG* and the Lower Saxony state government for their financial support for building the *Hannover Institute of Technology (HITec)* and the *Einstein-Elevator* (NI1450004, INST 187/624-1 FUGB).

## References

- DIN EN ISO 6892-1:2017-02, 2016. Metallische Werkstoffe - Zugversuch - Teil 1: Prüfverfahren bei Raumtemperatur (ISO\_6892-1:2016), Deutsche Fassung EN\_ISO\_6892-1:2016. DOI: 10.31030/2384831
- Liu, S., Shin, Y. C., 2019. Additive manufacturing of Ti6Al4V alloy: A review. *Materials and Design*, Elsevir. DOI: 10.1016/j.matdes.2018.107552
- Lotz, C., 2022. Untersuchungen zu Einflussfaktoren auf die Qualität von Experimenten unter Mikrogravitation im Einstein-Elevator. DOI: 10.15488/11713
- Lotz, C., Froböse, T., Wanner, A., Overmeyer, L., Ertmer, W., 2017. Einstein-Elevator: A New Facility for Research from  $\mu g$  to 5 g. DOI: 10.2478/gsr-2017-0007
- Lotz, C., Kämper, T., Berlin, H., Overmeyer, L., 2014. Innovative Drive and Guide Concept for Experiments under Microgravity in the Einstein-Elevator. ISBN: 978-3-944586-84-7
- Lotz, C., Piest, B., Rasel, E., Overmeyer, L., 2023. The Einstein-Elevator: Space Experiments at the new Hannover Center for Microgravity Research. *Europhysics News*, Volume 54, Number 2, 9-11. DOI: 10.1051/epn/2023201
- Lotz, C., Wessarges, Y., Hermsdorf, J., Ertmer, W., Overmeyer, L., 2018. Novel active driven drop tower facility for microgravity experiments investigating production technologies on the example of substrate-free additive manufacturing. *Advances in Space Research* 61 (2018) 1967–1974. DOI: 10.1016/j.asr.2018.01.010
- Mahamood, R. M., 2018. Laser Metal Deposition Process of Metals, Alloys, and Composite Materials. *Engineering Materials and Processes*. Springer International Publishing, Cham, 1st edition 2018 edition. DOI: 10.1007/978-3-319-64985-6
- Raupert, M., Pusch, M., Tahtali, E., Sperling, R., Heidt, A., Lotz, C., Katterfeld, A., Overmeyer, L., 2022. Laser Metal Deposition with Metal Powder in Microgravity, *Deutscher Luft- und Raumfahrtkongress 2022*, Dresden. DOI: 10.25967/570466
- Reitz, B., Lotz, C., Gerdes, N., Linke, S., Olsen, E., Pflieger, K., Sohr, S., Ernst, M., Taschner, P., Neumann, J., Stoll, E., Overmeyer, L., 2021. Additive Manufacturing Under Lunar Gravity and Microgravity, *Microgravity Science and Technology*, 33:25. DOI: 10.1007/s12217-021-09878-4
- Wunderlich, R. K., 2011. Surface Tension and Viscosity of Industrial Ti-Alloys measured by the Oscillating Drop Method on Board Parabolic Flights. *High Temperature Materials and Processes*, Vol 27, No. 6, pp. 401-412. <https://doi.org/10.1515/HTMP.2008.27.6.401>
- Yan, M., Yu, P., 2015. An Overview of Densification, Microstructure and Mechanical Property of Additively Manufactured Ti-6Al-4V - Comparison among Selective Laser Melting, Electron Beam Melting, Laser Metal Deposition and Selective Laser Sintering, and with Conventional Powder Metallurgy, *Sintering Techniques of Materials*, Chapter 5. DOI: 10.5772/59275
- Yang, Y., Song, B., Yang, Z., Song, G., Cai, Z., Guo, Z., 2016. The Refining Mechanism of Super Gravity on the Solidification Structure of Al-Cu Alloys. *Materials*. DOI: 10.3390/ma9121001